Review

Subsite-resolved molecular and epigenetic characterization of oral tongue squamous cell carcinoma: A systematic review and in silico genome-wide DNA methylation analysis

Bacem Othman[1,2,3,A–D,F], Omid Moztarzadeh[1,3,E,F], Lukas Hauer[1,E,F]

[1] Department of Stomatology, University Hospital Pilsen, Faculty of Medicine in Pilsen, Charles University, Pilsen, Czech Republic
[2] Biopticka Laboratory, Pilsen, Czech Republic
[3] Department of Anatomy, Faculty of Medicine in Pilsen, Charles University, Czech Republic

A – research concept and design; B – collection and/or assembly of data; C – data analysis and interpretation;
D – writing the article; E – critical revision of the article; F – final approval of the article

Dental and Medical Problems, ISSN 1644-387X (print), ISSN 2300-9020 (online) *Dent Med Probl*. 2026;63(5):1347–1361

Address for correspondence
Omid Moztarzadeh
E-mail: omid.moztarzadeh@lfp.cuni.cz

Funding sources
None declared

Conflict of interest
None declared

Acknowledgements
None declared

Received on August 2, 2026
Reviewed on August 30, 2026
Accepted on September 25, 2026

Published online on October 30, 2026

Abstract

Tongue squamous cell carcinoma (TSCC) arises predominantly in a human papillomavirus (HPV)-negative context, which shifts its pathogenesis away from the viral oncogene pathways involved in head and neck cancer.

Tongue-attributable literature was systematically reviewed in accordance with the Preferred Reporting Items for Systematic Reviews and Meta-Analyses (PRISMA) 2020 guidelines, and integrated with a primary genome-wide DNA methylation analysis of 112 SCC samples profiled using Illumina Infinium arrays, with comparisons against normal mucosa and SCCs arising at other head and neck subsites. The reported genes were functionally annotated using PANTHER, consolidated into interpretable thematic clusters, and assessed for evidence of druggability and methodological quality. The findings were synthesized narratively according to the functional theme, with the experimental system specified for each finding.

Fifty of the 197 extracted records could be confidently assigned to the tongue, while the remaining 147 were retained as an oral cavity comparator. Tongue SSC was distinguished by methylation and expression markers rather than by *PAX5* promoter methylation. Methylation was specifically associated with the tongue, together with a seven-gene expression signature (*MTFR1*, *C8orf33*, *OTUD6B*, *NUDCD1*, *PRKC1*, *ANO1*, and *PIK3CA*) derived from an HPV-associated comparator set.

Tongue SCC diverges from SCCs arising at other oral cavity subsites along an epigenetic rather than a mutational axis. Heterogeneity within TSCC reflects multiple molecular routes converging on a limited number of shared functional endpoints.

Limitations of the evidence: Human series were small and mostly retrospective; most study designs were preclinical and therefore provided indirect evidence; HPV, p53 and p16 ascertainment was incomplete; patient-tissue microRNA profiling relied on a single 50-pair series; and no outcomes were reported in a form that permitted data pooling.

Keywords: methylation, tongue squamous cell carcinoma, transcription factors, epigenetics, pseudogenes

Cite as
Othman B, Moztarzadeh O, Hauer L. Subsite-resolved molecular and epigenetic characterization of oral tongue squamous cell carcinoma: A systematic review and in silico genome-wide DNA methylation analysis. *Dent Med Probl.* 2026;63(5):1347–1361. doi:10.17219/dmp/240335

DOI
10.17219/dmp/240335

Copyright
Copyright by Author(s)
This is an article distributed under the terms of the Creative Commons Attribution 3.0 Unported (CC BY 3.0) (https://creativecommons.org/licenses/by/3.0/)

Highlights

- Genome-wide DNA methylation profiling revealed promoter methylation differences in tongue squamous cell carcinoma (TSCC) at loci also affected by rearrangements in fusion-positive oral cancer.
- Integrated systematic review and in silico analysis identified 19 genes shared between fusion-partner events and promoter hypermethylation across tumor subsets.
- Functional classification of 280 unique gene symbols into 13 consolidated PANTHER protein classes showed pathway-level convergence in TSCC.
- Convergent methylation targets highlight potential biomarkers for early diagnosis and prognosis in TSCC, although none has yet been validated against clinical endpoints.

Introduction

Squamous cell carcinoma (SCC) of the oral tongue is one of the most common malignancies of the oral cavity, and outcomes remain poor once the disease is locally advanced, recurrent or metastatic. Unlike SCC of the oropharynx, oral tongue SCC (OTSCC) is overwhelmingly human papillomavirus (HPV)-negative; therefore, its molecular pathogenesis must be sought outside the viral oncogene pathways that dominate much of the head and neck cancer literature.[1] Tongue tumors are nevertheless often grouped with SCCs arising at other oral cavity subsites, or with head and neck squamous cell carcinoma (HNSCC) as a whole.

The divergence from the oropharynx merits explanation on anatomical grounds, since the two subsites lie within a few centimeters of each other. Transforming papillomavirus infection depends on the access of virions to basal keratinocytes. The reticulated, discontinuous epithelium of the tonsillar and base-of-tongue crypts provides direct access to these cells, without the need for antecedent injury. In contrast, the oral tongue is covered by a continuous keratinizing stratified squamous epithelium overlying an intact basement membrane and a dense lamina propria. Access to the basal compartment at this subsite therefore depends on tissue injury. The crypt epithelium is further embedded in lymphoid tissue characterized by a locally tolerogenic immune milieu, which is permissive of viral persistence. Persistence at the oral tongue is correspondingly uncommon, and the detection of viral DNA at this subsite frequently reflects transient viral carriage.

Carcinogenesis at the oral tongue is dominated instead by tobacco- and alcohol-related field changes and, in a distinct subset of young never-smokers, by an etiology that remains unexplained. The practical consequence for the present synthesis is that p16 immunohistochemistry has no validated role as a surrogate marker of viral causation at this subsite.

Treating OTSCC, particularly non-HPV-related disease, presents significant therapeutic challenges. Conventional chemotherapeutic agents (cisplatin, paclitaxel, docetaxel, carboplatin, gemcitabine, fluorouracil, methotrexate, oxaliplatin, and doxorubicin) demonstrate limited efficacy as monotherapies, and are therefore often used in combination with immune checkpoint inhibitors (ICIs) (pembrolizumab, nivolumab, cemiplimab, atezolizumab, durvalumab, ipilimumab, camrelizumab, and toripalimab) or agents targeting epidermal growth factor receptor (EGFR) and vascular endothelial growth factor (VEGF) signaling (cetuximab, afatinib, erlotinib, bevacizumab, sorafenib, and lenvatinib), depending on the relevant biomarker profile, including positive immunohistochemical markers or the detection of *FGF3*/*FGF4* amplification.[2–5]

Still, no recurrent gene fusion has been reported in tongue-attributable series, and the fusion events available for comparison in this review derive from oral SCC records in which the tongue was not identified as a separate subsite. Denominators are unavailable for either group; therefore, no comparison of fusion frequency by subsite is made in this review.

Genetic alterations more broadly are sparsely reported in the tongue-restricted literature. Given this paucity of evidence, we reasoned that epigenetic mechanisms, and DNA methylation in particular, might account for a disproportionate share of TSCC pathogenesis.

Two research questions therefore structure the synthesis that follows. The first asks how the molecular profile of TSCC compares with that of SCC arising at other oral cavity subsites, and whether this comparison identifies alterations that are genuinely distinctive to the tongue. The second asks what accounts for the molecular heterogeneity observed within TSCC itself, and what contributions microRNAs, long non-coding RNAs, and pseudogenes make to this heterogeneity.

Methods

Systematic review

Protocol and vetted studies

This systematic review was conducted and is reported in accordance with the Preferred Reporting Items for Systematic Reviews and Meta-Analyses (PRISMA) 2020 statement. The review addressed which somatic, germline and

epigenetic alterations, and which consequent changes in gene and protein expression, have been reported in TSCC, and how these findings differ according to the experimental system in which they were generated. Eligibility was framed using a PECO (Population, Exposure, Comparator, and Outcome)-type structure adapted for molecular research. The population comprised SCC arising in the tongue, whether studied as human tumor tissue, patient-derived material, cell lines of tongue origin, or experimentally induced tongue carcinoma in animal models. The exposure was any reported molecular alteration, including somatic mutation, germline variant, copy number alteration, gene fusion, promoter or genome-wide methylation change, histone modification, differential mRNA, microRNA, long non-coding RNA or circular RNA expression, and differential protein expression or post-translational modification. The comparator, where present, was non-neoplastic tongue or oral mucosa, paired surgical margin tissue, premalignant lesions, or a less aggressive counterpart cell line or subline. Outcomes were the identity of the altered gene or gene product, the direction of the alteration, its functional consequence where tested, its association with clinical or pathological variables, and its reported druggability.

Studies were eligible if they reported original molecular data attributable to OTSCC and identified at least one gene, gene product or defined genomic region. Exclusion from the review altogether was applied to purely methodological work without disease-specific findings and to records without an available English full text. Ineligibility for the tongue cluster, as distinct from exclusion from the review, was applied to records without primary data, such as narrative reviews, editorials and conference abstracts without an accompanying dataset, to records on malignancy arising outside the tongue, and to records on non-neoplastic material. Records of these three kinds were retained in the comparator cluster as the oral-cavity and head and neck background for interpretation of tongue-attributable findings. Comparator records were never counted toward tongue-specific evidence and are identified as comparator at every point of use. No restriction was placed on sample size or study design. Records published before 2005 were not retrieved. The PRISMA 2020 flow diagram is shown in Fig. 1.

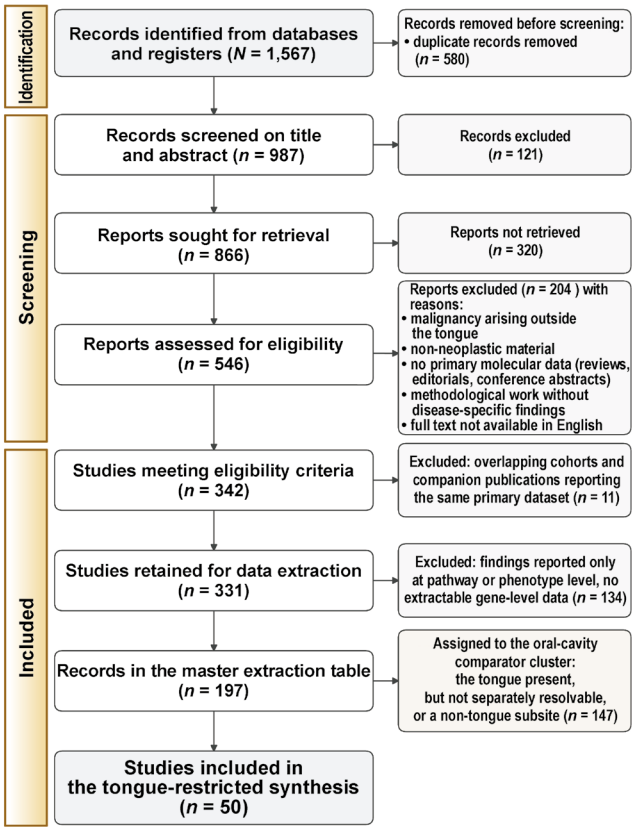


Fig. 1. PRISMA 2020 flow diagram for study identification, screening and inclusion

Search strategy and study selection

Electronic search was performed in Scopus, the Web of Science, Ovid, and PubMed from 2005 to 2025. The search combined controlled vocabulary with free-text terms across anatomical site, histology and molecular alteration. The anatomical block included tongue, oral tongue, lingual and their variants; the histological block included squamous cell carcinoma, carcinoma, and the abbreviations TSCC, OTSCC, SCCOT, OSCC and HNSCC; the molecular block included mutation, methylation, copy number, amplification, deletion, gene expression, microRNA, long non-coding RNA, proteomic, transcriptomic, exome and genome sequencing. Blocks were combined with AND, and terms within blocks with OR. The reference lists of retrieved articles and of relevant reviews were hand-searched, and forward citation tracking was performed on studies retained at full-text stage.

Title-and-abstract screening and full-text assessment were performed independently by two reviewers (B.O. and O.M.), with disagreement resolved by discussion against the eligibility criteria. Formal risk-of-bias instruments were not applied. The included literature is predominantly laboratory-based molecular work, for which no validated instrument of this kind exists. Methodological confidence was recorded instead at extraction as 3 items: the design category of the study; the presence or absence of an internal comparator; and the presence or absence of orthogonal validation of the reported alteration.

The search yielded 1,567 records. After the removal of duplicates, 987 records were screened on title and abstract, of which 866 were sought for retrieval. Of these, 546 reports were obtained and assessed against the full eligibility criteria, leaving 342 studies meeting the criteria, of which 331 were retained after resolution of overlapping cohorts and companion publications reporting the same primary dataset. Of these 331 studies, 197 reported gene-level molecular data in a form permitting structured extraction and constitute the master extraction table on

which the synthesis is based; the remaining 134 reported findings only at pathway or phenotype level and were not extracted. Fifty of the 197 extracted records reported findings attributable to the tongue and constitute the tongue cluster analyzed; the remaining 147 constitute the oral-cavity comparator cluster.

Data extraction and classification of the study design

Data were extracted into a purpose-built master table using a standardized form piloted on a random sample of 10 studies. The following items were recorded for every included study: first author and year; study design; anatomical site and histological type as reported by the authors; number of patients, specimens or cell lines; HPV status; p53 status; p16 status; whether immunohistochemistry was performed and for which targets; the genetic or molecular method used; the class of molecular alteration; the output gene or genes; the key molecular findings in narrative form; the nature of the biological material as primary, control or secondary; and the digital object identifier of the source publication. Where a study reported findings for more than one anatomical site or experimental system, each was recorded separately so that site- and system-specific attribution was preserved. Extraction was performed by two reviewers (B.O. and O.M.).

Since the interpretive weight of a molecular finding depends on the system in which it was generated, every study was assigned to one or more of 4 design categories. Human tissue studies analyzed primary patient material, including retrospective and prospective cohorts, paired tumor and margin designs, tissue microarrays, liquid biopsy and patient-derived organoids. In vitro studies used established or patient-derived cell lines, three-dimensional (3D) organotypic cultures, extracellular vesicle preparations or cell-free systems. In vivo studies used genetically engineered mouse models, chemically induced carcinogenesis such as 4-nitroquinoline 1-oxide (4NQO) exposure, subcutaneous or orthotopic xenografts, syngeneic implantation, or non-murine animal systems. In silico studies analyzed public repositories such as The Cancer Genome Atlas (TCGA) or the Gene Expression Omnibus (GEO), or performed meta-analysis, network reconstruction or predictive modelling without generating primary data. All applicable categories were retained.

Tongue cluster and oral-cavity comparator

The cohort was defined by the authors as tongue squamous cell carcinoma (TSCC, OTSCC or SCCOT); the tumors were induced in, or the tissue sampled from, the tongue in an animal model; a specific finding was reported for the tongue subsite within a larger oral cavity or head and neck cohort; or the experimental material was a cell line of documented tongue origin. Cell lines accepted as tongue-derived were SCC-4, SCC-9, SCC-15, SCC-25, HSC-3, CAL-27, SAS, Tca8113, UM1 and UM2, together with the murine MOC-L and MTCQ series derived from carcinogen-induced tongue tumors. Carcinomas of the base of tongue and of the tonsil were classified as oropharyngeal and excluded from the tongue cluster, because their etiology, HPV association and molecular profile diverge substantially from those of the oral tongue. Carcinomas of the gingivobuccal complex, gingiva, buccal mucosa, floor of mouth, larynx, esophagus and salivary glands were likewise excluded.

Studies of oral cavity or head and neck SCC in which tongue tumors were present but not separately resolvable were not discarded. They were assigned to a comparator cluster and retained as the oral-cavity control against which tongue-specific findings were read, allowing alterations distinctive to the tongue to be distinguished from those general to oral squamous carcinogenesis. Findings drawn from the comparator cluster are identified as such wherever they appear and are never presented as tongue-specific evidence.

Functional annotation of output genes

All genes and gene products recorded in the extraction table were consolidated into a single non-redundant list and submitted to the PANTHER classification system for assignment to protein class. Gene symbols were reconciled against current HGNC nomenclature before submission, and symbols reported under superseded or non-standard forms were mapped to their approved equivalents, while the original designation was preserved in the extraction table. Annotation returned 308 gene assignments across 84 protein classes. A single symbol may receive more than one class assignment, so the 308 assignments correspond to a smaller number of distinct symbols. The removal of duplicate assignments and of symbols not reconcilable to current HGNC nomenclature left 280 unique gene symbols. The largest single category was Unknown, comprising 62 genes for which PANTHER returned no assignment, followed by transmembrane signal receptors (15), non-receptor serine/threonine protein kinases (12) and a residual Unclassified category (10), with a further 34 classes containing a single gene each. Since a synthesis organized around 84 classes would be neither readable nor interpretable, and because many classes are functionally adjacent, the PANTHER output was used as the basis for a smaller number of functional themes. Genes returned as Unknown or Unclassified were assigned to a theme based on the function attributed to them in the source study.

Transcription factors and transcriptional regulators were treated as a distinct analytical focus. They were distributed across 12 separate PANTHER classes – homeodomain, DNA-binding, basic helix-loop-helix, C2H2 zinc finger, winged helix/forkhead, Rel homology, HMG box, P53-like, Runt, basic leucine zipper and zinc finger transcription

factors, together with transcription cofactors – comprising 38 gene assignments and forming the single largest functional grouping once the dispersal across classes is reversed. This dispersal is an artefact of the PANTHER structural taxonomy, and the classes were reconsolidated for synthesis so that transcriptional regulation could be assessed as a coherent axis.

Druggability annotation

Each study was classified according to whether druggability was addressed and at what level of evidence. Pharmacological testing, in which a defined compound was administered to a biological system and an effect measured; target nomination, in which a gene or pathway was proposed as actionable without experimental testing; and no assessment. For studies in the first category, the compound, its molecular target, the system in which it was tested, and the direction of the observed effect were recorded, together with any result running counter to the expected pharmacological direction.

Fusion-partner gene set used as the genetic comparator

The genetic comparator shown in Fig. 2 is a gene set where no fusion calling was performed de novo for this review. Fusion transcripts recorded for fusion-positive oral squamous cell carcinoma were split into their constituent 5' and 3' partner genes. Partner symbols were reconciled to the current HGNC nomenclature, so that genes altered by rearrangement and genes altered by promoter methylation occupy one symbol space. Fusion counts carry no denominator in this design and are not used to estimate fusion frequency at any subsite. Comparison against the methylation output is made at the level of gene identity alone.

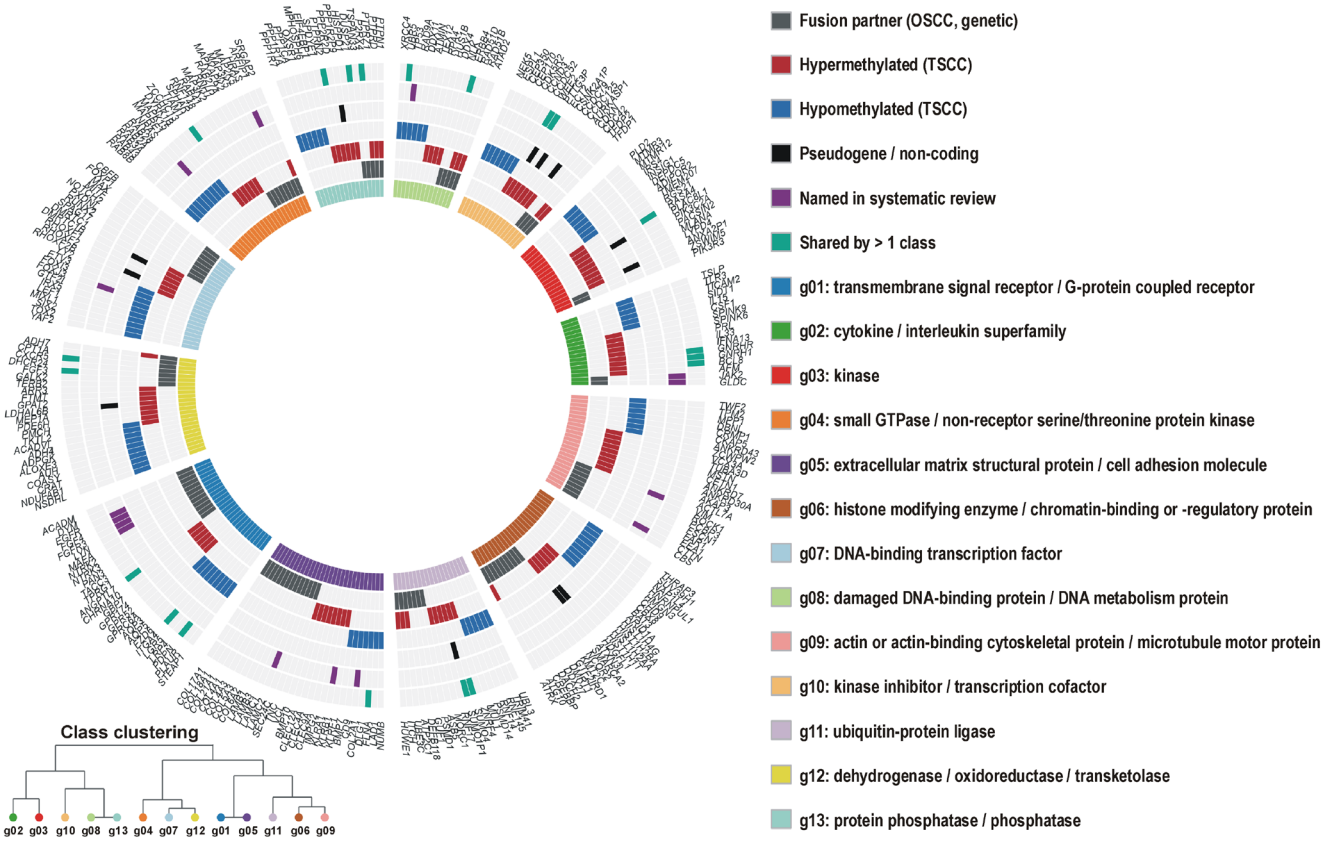


Fig. 2. Convergence of genetic and epigenetic alteration on shared functional classes in tongue squamous cell carcinoma (TSCC)

Each radial sector represents one gene symbol (n = 280). Fusion transcripts detected in fusion-positive oral SSC were split into their constituent partner genes, so that genes altered by rearrangement and genes altered by methylation occupy the same symbol space and can be compared directly. Sectors are grouped into 13 PANTHER protein classes and separated by gaps. Concentric rings indicate, from the center outward: (1) PANTHER class, color-coded as in the key; (2) presence as a fusion partner in fusion-positive oral SCC, which serves as the genetic comparator; (3) promoter hypermethylation in fusion-negative, mutation-negative TSCC; (4) promoter hypomethylation in the same tumors; (5) annotation as a pseudogene or non-coding transcript; (6) the gene is also named in the systematic-review gene set; and (7) the gene is assigned to more than one PANTHER class, in which case only its first class in cluster order is shown. Pale grey denotes the absence of that feature. Gene symbols are set radially outside the outermost ring. The inset dendrogram orders the 13 classes by Ward D2 clustering (Euclidean distance) of their alteration-mode composition – the proportion of each class's entries contributed by fusion, hypermethylation and hypomethylation, together with class size – so that classes group by how they are altered; membership-based clustering was not informative because the 13 gene sets are almost entirely disjoint. Nineteen genes carry both a fusion partner mark and a hypermethylation mark (*ADH7*, *ATAD2*, *ATRX*, *CXCR5*, *ERBB4*, *HUWE1*, *ITCH*, *P2RX4*, *PTPN1*, *PTPRD*, *PTPRN2*, *PTPRZ1*, *RAD51B*, *RAD51D*, *SRGAP2*, *TFDP1*, *TFDP2*, *TIAM1*, and *UBE3C*), identifying loci disrupted genetically in one tumor group and epigenetically in the other. No gene was both a fusion partner and hypomethylated. Methylation calls derive from Infinium array IDAT files retrieved from the Gene Expression Omnibus and processed.

In silico genome-wide DNA methylation analysis

Dataset selection

In addition to the systematic review, a primary bioinformatic analysis of genome-wide DNA methylation was performed to characterize epigenetically OTSCC from OSCC. Raw intensity data (IDAT) files for Illumina Infinium methylation arrays were retrieved from the Gene Expression Omnibus (GEO). Every contributing series, and the disposition of every array within it, is listed at sample level in Supplementary Table S2. That table records, for each array, the GEO series, the GSM accession, the array platform, the anatomical subsite, the tumor or normal status, the sex and the age where deposited, the sentrix slide and position, and the final analytical group. Series were selected in preference to processed beta matrices so that preprocessing could be harmonized across submissions, and in preference to mixed head and neck cohorts so that the tongue could be resolved as a discrete subsite. The largest contribution was GSE79556 (n = 83; GSM2098204–GSM2098286), a single-institution series of comprehensively annotated OTSCCs profiled on the HumanMethylation450 BeadChip (GPL13534). This was supplemented by 6 oral tongue carcinoma arrays from GSE210443 (GSM6430352, 6430354, 6430356, 6430358, 6430360 and 6430362), profiled on the higher-resolution MethylationEPIC BeadChip (GPL21145) covering approximately 850,000 loci, which extends coverage beyond the 450K design and provides a platform-independent check on the principal cohort.

Samples were eligible where the array was generated from primary, treatment-naive human tissue; where raw IDAT files were available so that preprocessing could be harmonized across series; and where the anatomical subsite was stated unambiguously in the sample metadata. Arrays from cell lines, from recurrent or post-treatment specimens, and from samples whose subsite could not be determined were not used. Within the tongue group, only cases negative for recurrent driver gene fusions and for recurrent somatic driver mutations were analyzed, so that methylation change could be examined in tumors not otherwise accounted for by a genetic driver; fusion-positive OSCC cases were retained separately as the genetic-driver comparator and accessioned in Supplementary Table S2 with their series of origin, their platform and their subsite as deposited. Anatomical group and series of origin are not orthogonal in this design. GSE79556 contributes oral tongue carcinoma only.

Preprocessing

The IDAT files were imported in R with the minfi package using read.metharray.exp, retaining the red and green channel intensities without prior transformation. Since the contributing series span 2 generations of the Infinium platform, arrays were harmonized before any quantitative comparison: HumanMethylation450 (450K) and MethylationEPIC (EPIC) data were combined using combineArrays, which reduces the feature set to the probes present on both designs, and all downstream analysis was restricted to that common set. Background correction and dye-bias equalization were performed with single-sample Noob (ssNoob), which is applied independently to each array and is therefore the appropriate choice when data from different platforms and different submission batches are to be merged; array-dependent methods such as standard Noob or SWAN were avoided for this reason. Methylation was expressed as beta values, defined as the ratio of methylated to total (methylated plus unmethylated plus 100) signal, for description and visualization, and as M values, the base-two logit of beta, for all statistical testing, since M values are approximately homoscedastic across the methylation range whereas beta values are not.

Normalization

Following ssNoob, between-array normalization was performed by functional normalization (preprocessFunnorm) using the first two principal components of the internal control probes as covariates. Functional normalization was preferred to quantile-based methods, because the comparison of interest is between tumor and normal tissue, where global methylation differences are expected to be genuine and quantile normalization would suppress them. Residual Infinium type I / type II design bias was then corrected with beta-mixture quantile normalization (BMIQ). The effect of each normalization step was inspected on density plots of the beta distribution, on multidimensional scaling plots of the 1,000 most variable positions, and on the control probe metrics, both before and after correction.

Probe filtering

Probes were removed, in order, where the detection p-value exceeded 0.01 in any sample; where fewer than 3 beads contributed in more than 5% of samples; where the probe interrogates a non-CpG site; where the probe overlaps a known single nucleotide polymorphism at the target CpG or the single-base extension position at a minor allele frequency of at least 0.05, using dropLociWithSnps; where the probe has been reported as cross-reactive or multi-mapping in the published masking lists for the 450K and EPIC arrays; and where the probe maps to a sex chromosome, since sex was not the exposure of interest and unbalanced sex distribution across groups would otherwise contribute spurious signal. Samples were excluded where the mean detection p-value exceeded 0.01 across all probes, or where more than 1% of probes failed detection.

Batch correction and cell composition

As the samples derive from independent GEO submissions processed in different laboratories, on 2 array generations and across multiple slides, batch effect is the dominant technical risk in this design and was addressed. Sources of unwanted variation were first quantified by singular value decomposition against the available technical and biological covariates, testing the association of each principal component with series of origin, array platform, sentrix slide and sentrix position, alongside analytical group, sex and age. Correction was then applied to M values with ComBat, using series of origin as the batch variable and including the analytical group in the model matrix so that the biological contrast was protected from removal; slide was modelled as a nested second batch term where singular value decomposition indicated residual slide-associated variance. Correction was verified by repeating the decomposition on the adjusted matrix and by re-examining the multidimensional scaling plot. ComBat removes variance attributable to the batch variable, and it cannot recover a biological effect where the biological group and the batch are collinear. In this design the tongue carcinoma group derives almost entirely from one series on one platform, so analytical group and series of origin are close to structurally confounded for the tongue against other subsites contrasts. The tongue against normal mucosa contrast is not affected to the same degree, since normal and tumor arrays are contributed within series. Since solid tumor and mucosal samples are cellular mixtures, epithelial, fibroblast and immune cell fractions were estimated by reference-based deconvolution with the hierarchical EpiDISH procedure and included as covariates in the differential methylation model, so that differences in tumor purity and immune infiltrate are not read as methylation differences.

Quality control

Quality control was applied at 3 points. Before preprocessing, the median methylated and unmethylated intensities of each array were plotted and arrays falling below the conventional threshold were flagged; the 17 Illumina control probe categories, covering bisulphite conversion for both Infinium chemistries, staining, extension, hybridization, target removal, specificity and negative controls, were inspected on the standard qcReport. After preprocessing, genotypic sex was predicted from the median total intensity of the X and Y chromosomes and compared with the sex recorded in the sample metadata, with discordant arrays excluded (Supplementary Table S3). The 65 (450K) or 59 (EPIC) SNP-targeting rs probes were used to check for unrecognized duplicate samples across the contributing series, since overlapping patient material between public submissions would otherwise inflate significance; any pair exceeding a genotype correlation of 0.90 was reduced to a single representative array. After filtering, the beta distribution of every retained array was inspected for bimodality, and arrays with distorted distributions were removed.

Differential methylation and functional mapping

Differentially methylated positions were identified by fitting a linear model to the batch-corrected M values with *limma*, using an analytical group term and adjusting for age, sex and the estimated cell fractions, with empirical Bayes moderation of the variance estimates. Three contrasts were specified. The 1st set tongue carcinoma against normal tongue and oral mucosa. The 2nd set tongue carcinoma against carcinoma of other oral cavity subsites, namely gingivobuccal, buccal, gingival, palatal and floor-of-mouth carcinoma, and this contrast addresses the review question directly. The 3rd set tongue carcinoma against carcinoma of head and neck subsites outside the oral cavity, namely oropharyngeal, laryngeal and sinonasal carcinoma, and it is reported as a secondary comparison. Positions were considered significant at a Benjamini-Hochberg adjusted p-value below 0.05 together with an absolute mean beta difference greater than 0.3, a threshold chosen to exclude changes too small to be biologically meaningful or reliably measurable on array platforms. Differentially methylated regions were called with DMRcate using a Gaussian kernel bandwidth of 1,000 base pairs and a scaling factor of 2, requiring at least three constituent CpGs and a region-level false discovery rate below 0.05. Probes were annotated to genes and to genomic context (TSS1500, TSS200, 5' UTR, first exon, gene body, 3' UTR; island, shore, shelf, open sea) using the manufacturer manifest, and gene-level hypermethylation or hypomethylation was assigned where concordant differentially methylated positions fell within the promoter region, defined as TSS1500, TSS200, the 5' UTR or the first exon. Genes unique to tongue carcinoma after comparator filtering were clustered with PANTHER and mapped onto the same functional themes as the review, and set against the fusion-driven alterations reported in oral cavity carcinoma, so that genetic and epigenetic routes to the disruption of each functional axis could be compared directly.

Software

All analysis was performed in R version 4.3.2 using Bioconductor release 3.18, with *minfi* 1.48.0 for import, preprocessing and quality control; the IlluminaHumanMethylation450kanno.ilmn12.hg19 and IlluminaHumanMethylationEPICanno.ilm10b4.hg19 annotation packages; wateRmelon 2.8.0 for BMIQ; *sva* 3.50.0 for ComBat; EpiDISH 2.18.0 for cell type deconvolution; limma 3.58.1 for differential testing; DMRcate 2.16.0 for region calling; and missMethyl 1.36.0 for probe-number-corrected enrichment testing.

Results

Oral tongue squamous cell carcinoma

Composition and study disposition

Of the 197 records held in the master extraction table, 50 reported molecular findings attributable to the tongue with confidence and were retained for synthesis. The remaining 147 records were assigned to the oral-cavity comparator cluster. These comprised oral-cavity or head and neck cohorts in which tongue tumors were present, but not separately resolvable; carcinomas of non-tongue subsites (gingivobuccal, gingival, buccal pouch, oropharyngeal and tonsillar, laryngeal, esophageal and salivary gland); malignancies of other organs; non-neoplastic studies of the tongue or oral cavity; and narrative reviews without primary data. Records of these kinds were ineligible for the tongue cluster and were retained as a comparator.

Distribution of study designs

Twenty-eight studies used in vitro systems, whether established or patient-derived cell lines, 3D organotypic cultures or extracellular vesicle preparations; 21 included an in vivo component, most often 4NQO carcinogenesis in genetically modified mice, but also subcutaneous and orthotopic xenografts, syngeneic implantation, a rat carcinogenesis model and a zebrafish embryo model; 14 analyzed human tongue tissue in retrospective cohorts or paired tumor-margin designs; and 9 were wholly or partly in silico. Several studies spanned more than one category, and the strongest reports combined human tissue with functional validation. Human cohorts were generally small: the largest tongue-specific series were 93 OSCCs with tongue-stratified analysis,[6] 68 early-stage TSCC primary tumors,[7] 60 TSCC specimens[8] and 50 tumor-margin pairs,[9] while genome-wide methylation profiling of oral tongue carcinoma was performed on only 6 paired tissue-saliva samples before validation against TCGA.[10]

Molecular alterations by functional axis

The p53 axis, cell-cycle control and replicative immortality

Alterations converging on p53 were reported across every study design. A germline family study combined with an Mdm4 knock-in mouse showed that the *MDM4* p.T454M substitution paradoxically increases p53 activity and produces telomere shortening and bone marrow failure, with TSCC and acute myeloid leukemia occurring in affected family members.[11] In murine tongue tumor cell lines derived from 4NQO-treated transgenic animals, a missense *TP53* mutation in the DNA-binding domain co-occurred with miR-211 upregulation in the most metastatic line.[12] Conditional mouse genetics established that p53 loss is permissive as inducible K-rasG12D combined with Trp53 deficiency and PPP6C (PP6) deletion produced tongue carcinoma in situ within approx. 2 weeks, through enhanced ERK-ELK1-FOS and AKT-4EBP1 signaling, DNA double-strand breaks and NF-kappaB activation,[13] while K14-CreERtam-driven K-rasG12D with conditional p53 loss drove oral and tongue carcinoma via mTOR pathway activation.[14]

Downstream cell-cycle effectors were addressed mainly in vitro. In the tongue-derived SCC-9 line, eugenol modulated p21, p27 and cyclin D1 to impose G0/G1 arrest while downregulating *MMP1* and *MMP3*[15]; the parallel silencing of p16 (*CDKN2A*) and p21 by *EZH2* is described with the chromatin evidence. Replicative immortality was addressed in a pan-cancer sequencing survey of 1,230 tumors across 60 types, which placed TSCC among the TERT-high tumor types with promoter mutation frequencies of at least 15%, and showed *TERT* promoter and *ATRX* mutations to be mutually exclusive.[16]

Receptor tyrosine kinase, kinase and phosphatase signaling

Receptor-proximal signaling was interrogated almost entirely in cell line systems. Triple inhibition of FAK, ErbB-family receptors and AXL in 2D and 3D spheroid cultures of head and neck cancer lines including tongue carcinoma downregulated Axl, FAK and N-cadherin while restoring E-cadherin, reversing the mesenchymal phenotype.[17] Focal adhesion kinase (PTK2) showed progressive overexpression across the successive stages of 4NQO-induced rat tongue carcinogenesis, making it one of the few kinases with staged in vivo evidence.[18] In CAL-27-derived clones, de novo integrin alphaVbeta3 expression conferred multidrug resistance through loss of Src phosphorylation at Y418, with ILK and integrin beta5 knockdown used to dissect the mechanism; the Src inhibitors dasatinib and PP2 reproduced.[19]

PI3K-AKT input was reported through 2 distinct upstream mechanisms. Sp1 overexpression in tongue cancer cell lines transcriptionally repressed PTEN through an HDAC1-dependent mechanism, increasing AKT phosphorylation and migratory capacity,[20] while in TSCC tissue and matched cell lines the long non-coding RNA *LINC00152* sponged miR-193b-3p to activate PI3K/AKT signaling.[21] The loss of the secreted MAPK modulator *CHRDL1* in CAL-27 cells and patient tissue activated ERK1/2, p38 and JNK to drive epithelial-mesenchymal transition, and its re-expression suppressed pulmonary colonization in a tail-vein metastasis model.[22] *FOXO4* was downregulated and under negative control by peroxiredoxin-1 in tongue tissue, cell lines and a 4NQO mouse model, with proximity ligation used to demonstrate the interaction.[23] In head and neck cancer lines including tongue lines with mouse xenograft validation, the BH3-mimetic gossypol reduced Bcl-2 and ErbB2, inhibited *ERK1/2* and *AKT*, and activated p38 and JNK.[24]

Developmental signaling: Wnt, Notch, Hedgehog and Hippo

Wnt/beta-catenin was the most frequently implicated developmental pathway. In APCmin/+ and Patched+/– mice studied alongside human tongue tissue, APC mutation activated Wnt/beta-catenin signaling and the normal Shh- and JAG2-mediated negative feedback was lost in established carcinoma.[25] A zebrafish embryo model combined with the tongue carcinoma line SAS showed that loss of LZAP raises nuclear beta-catenin through inhibitory phosphorylation of *GSK3*.[26] In SCC-9 transfectants, the balance between plakoglobin and beta-catenin governed Bcl-2 expression and therefore apoptotic threshold, with concomitant changes in N-cadherin and alpha-catenin.[27] The secreted Wnt antagonist *SFRP1* was downregulated in TSCC on combined GEO and TCGA mining with RT-PCR, Western blot, immunohistochemical and animal validation.[28]

Notch signaling behaved inconsistently between model systems. Stable transfection of the intracellular Notch1 domain into Tca8113 tongue carcinoma cells suppressed growth and induced apoptosis and cell-cycle arrest, with accompanying changes in beta-catenin, p21WAF1/CIP1, p53, Skp2 and Bcl-2, supporting a tumor-suppressive role.[29] In contrast, whole-exome and transcriptome sequencing of 68 early-stage TSCC tumors found *NOTCH1* somatically amplified and overexpressed with an inactivating mutation rate of only 4 per cent, and gamma-secretase inhibition with shRNA knockdown supported an oncogenic role.[7] Hippo pathway disruption produced the most rapid tumor phenotype recorded in any included model: tongue-specific Mob1a/b knockout mice developed carcinoma in situ by two weeks and invasive carcinoma by four weeks through *YAP1* hyperactivation; *YAP1* activation was detectable in human precancerous tongue dysplasia where it correlated with reduced survival, and both siRNA and pharmacological *YAP1* inhibition blocked tumor onset.[30]

Adhesion, epithelial–mesenchymal transition and invasion

Epithelial–mesenchymal transition was consistently reported, but studied almost exclusively in cell lines and paired-line comparisons. HMGA2 overexpression in the SCC-15 line and in TSCC tissue drove EMT with Twist and vimentin upregulation and E-cadherin loss.[31] In paired cell lines established from a primary tongue lesion and its nodal metastasis, vimentin overexpression maintained the mesenchymal phenotype and in vivo tumorigenicity, with reciprocal loss of keratins K13, K14 and K15.[32] The comparison of the high-invasion UM1 and low-invasion UM2 TSCC lines identified downregulation of MTUS1/ATIP3a, which normally restrains ERK1/2 signaling, with downstream Snai2 (SLUG) and vimentin induction.[33] Hypoxia contributed directly: cobalt chloride treatment of OTSCC cells induced *FNDC3B* through HIF-1alpha, and FNDC3B knockdown suppressed the EMT and metastatic phenotype.[34]

RNA sequencing across five increasingly invasive SCC-9-derived lines identified *PIGG* and *SLC8B1* as novel metastasis markers and nominated MYH14, ANGPTL4, PPARD and ENPP1 as interactome-predicted druggable hits, although no compound was tested.[35] Multi-omic profiling of extracellular vesicles from the primary SCC-9 line and its metastatic LN1 derivative identified 7 hub proteins – *ALDH7A1*, *CAD*, *CANT1*, *GOT1*, *MTHFD1*, *PYGB*, and *SARS* – whose low abundance correlated with reduced survival on public database validation.[36] In SCC-25 cells, *TTLL12* overexpression protected tubulin from nitrotyrosine-induced dysfunction and enhanced survival, and nocodazole proved more effective than paclitaxel in this regard.[37]

Copy number architecture

Only one study characterized genome-wide copy number in a purely tongue-derived resource. Microarray profiling of copy number and expression across 18 OTSCC cell lines identified high-level amplifications at 6q12-q14, 9p24, 11p12-p13, 11q13 and 14q24, and nominated *CD109*, *MYO6*, *JAK2*, *CD274*, *TRAF6*, *CD44*, *FADD*, and *CTTN* as amplified candidate targets.[38]

Chromatin regulation and DNA methylation

Polycomb-mediated repression was addressed by3 studies with divergent results, and the direction of effect depended on the model. In tongue cancer tissue, cell lines and xenografts, *EZH2* overexpression silenced p16, p21 and E-cadherin through *H3K27* trimethylation and modulated CD44, and the *EZH2* inhibitor DZNep combined with 5-fluorouracil produced tumor suppression.[39] In direct contrast, tamoxifen-regulated conditional *EZH2* knockout in the tongue epithelium of 4NQO-treated mice increased the incidence of invasive carcinoma and high-grade neoplasia, a context-dependent result carrying an explicit cautionary implication for EZH2-directed therapy.[40] BMI1 overexpression in tongue basal stem cells of 4NQO-treated KrTB transgenic mice increased tumor severity and drove glycolytic reprogramming, with coordinate changes in *SOX9*, *HIF1A*, *MMP9*, *INHBB*, and *MYOF*.[41]

Methylation studies were the most tongue-specific body of evidence in the dataset. Genome-wide profiling of 6 paired oral tongue carcinoma tissue and saliva samples using the MethylationEPIC array, validated against the TCGA oral tongue cohort, identified 25,890 differentially methylated CpG sites and 6 salivary hypermethylated genes – *A2BP1* (*RBFOX1*), *ANK1*, *ALDH1A2*, *GFRA1*, *TTYH1* and *PDE4B* – each achieving diagnostic accuracy of at least 0.800 by area under the curve (AUC).[10]

Methylation-based enhancer and transcription factor binding site analysis of SCC of the oral tongue identified master regulator transcription factors activated in association with invasiveness, metastasis, EMT and poor prognosis, and others downregulated in association with tumor suppression, although individual factors were not enumerated.[42] Within a 93-patient oral SCC cohort analyzed by MS-MLPA, PAX5 promoter methylation was specifically associated with the tongue subsite, while WT1, *MSH6* and GATA5 methylation carried prognostic weight across the cohort.[6]

Metabolic reprogramming, hypoxia and ferroptosis

Metabolic findings clustered around glycolysis and the hypoxic response and were derived predominantly from transgenic mouse models. The BMI1 tongue stem cell model coupled transcriptomic and metabolomic evidence of glycolytic shift with induction of *SLC2A1* (*GLUT1*), *PKM*, *LDHA* and *HK2*.[41] Caveolin-2 upregulation in intratumoral nerves of 4NQO-treated global and cell-type-specific Cav2 knockout mice drove tumor-nerve crosstalk together with metabolic reprogramming, assessed by orthotopic implantation and metabolic profiling.[43] A bioinformatic analysis with immunohistochemical validation in 60 TSCC specimens identified the ferroptosis-related prognostic genes *CA9*, *TNFAIP3* and *NRAS*, enriched for ECM-receptor interaction and IL-17 signaling.[8]

Immune, inflammatory and neural microenvironment

Microenvironmental findings were reported almost entirely from in vivo systems. Loss of the endoribonuclease N4BP1 in 4NQO-treated knockout mice arrested early carcinogenic transformation and prevented tumor formation altogether, against an 86% tumor incidence in wild-type animals, with CCL2 and GM-CSF implicated by single-cell and bulk transcriptomic profiling.[44] Dietary sodium nitrite induced a macrophage-mimicry phenotype switch in TSCC cells through a *CREB1–CD68* axis that promoted lymphatic metastasis, and a CREB1-specific inhibitor reversed the effect.[45] In syngeneic murine tongue carcinoma lines carrying complex p53 alterations, oncogenic miR-134 was associated with low E-cadherin, and the model was used to test cisplatin combined with anti-PD-L1 blockade.[46] Papillomavirus infection with MmuPV1 synergized with 4NQO exposure to produce invasive tongue carcinoma in both immunodeficient and immunocompetent mice, establishing viral oncogene activity as a cofactor.[47]

Non-coding RNA regulation

Non-coding RNA findings were distributed across every tier of evidence and were exclusively microRNA- and long non-coding RNA-mediated; no pseudogene or circular RNA evidence was recovered from tongue-attributable studies. The strongest microRNA evidence came from in vivo work. In K14-EGFP-miR-211 transgenic mice exposed to 4NQO, miR-211 suppressed TCF12 and thereby induced *FAM213A*, an axis corroborated against TCGA.[48] The same microRNA reappeared alongside miR-196b in murine tongue tumor cell lines derived from 4NQO-treated animals, where miR-211 was highest in the most metastatic line and co-occurred with a DNA-binding-domain TP53 missense mutation, and where cisplatin treatment reduced miR-196b expression in xenografts.[12] In syngeneic murine tongue carcinoma, miR-134 behaved as an oncogenic microRNA associated with low E-cadherin expression.[46]

Two microRNA axes were linked directly to treatment response. In a multicenter TSCC cohort with in vitro and in vivo validation, a BRCA1–miR-593-5p–MFF axis regulated mitochondrial fission and cisplatin sensitivity, and was significantly associated with both cisplatin response and survival.[49] In a 3D organotypic invasion model using the highly invasive HSC-3 line and SCC-15, combined with laser-capture microdissection, mass spectrometry proteomics and miRNA microarray, miR-498 and miR-940 acted through focal adhesion and ECM-receptor interaction pathways alongside 67 differentially expressed proteins.[50] Moreover, miR-124-3 and miR-769 target-gene networks converged ECM-receptor interaction, focal adhesion, protein digestion/absorption, and AGE-RAGE signaling.[51]

Patient-tissue profiling was limited to a single series. Comparison of 50 tongue tumors against paired marginal tissue found miR-184 and miR-378 upregulated and miR-497 and miR-506 downregulated, with miR-103 additionally differentially expressed.[9] On the long non-coding RNA side, LINC00152 sponged miR-193b-3p in TSCC tissue and matched cell lines to activate PI3K/AKT signaling,[21] and integrated competing-endogenous-RNA network analysis of TCGA and GEO TSCC data identified 15 differentially expressed mRNAs, 1 microRNA and 2 long non-coding RNAs of prognostic relevance, resolving TSCC into basal and differentiated molecular subtypes, the differentiated subtype being associated with lower alcohol exposure and better overall survival.[52]

Mixed OSCC cohorts have described a TP53-linked set comprising miR-34a, miR-99a, miR-143, miR-373, miR-380-5p and miR-504, with miR-99a acting through AKT/mTOR[53]; a diagnostic panel of miR-21, miR-125b-2*, miR-138, miR-155, miR-184 and miR-205[54]; downregulation of let-7a, let-7d, let-7f and miR-16 with variable upregulation of miR-29b, miR-142-3p, miR-144, miR-203, miR-223 and miR-1275[55]; and a *CDK2AP1* (DOC1)-directed set of miR-21-5p, miR-23b-3p, miR-26b-5p, miR-93-5p and miR-155-5p.[56] The only circular RNA evidence anywhere in the extraction table is likewise from the comparator cluster, where circRNA-102450 sponges miR-1178 in OSCC.[57] Only miR-184 is common to the tongue-specific and comparator lists, which indicates that the microRNA literature has not been resolved by subsite. One microRNA

acts on many transcripts, and one transcript is acted on by many microRNAs, so a measured effect on a named pathway does not establish selective control of that pathway through the microRNA concerned.

Subsite- and age-stratified expression analyses

Two secondary analyses addressed the tongue explicitly as a distinct subsite. A meta-analysis of 8 public microarray datasets with TCGA survival validation identified a tongue-specific gene set comprising *MTFR1*, *C8ORF33*, *OTUD6B*, *NUDCD1*, *PRKC1*, *ANO1*, and *PIK3CA*, distinguishing it from the HPV-associated set of *RPP25*, *NUDCD2* and *NOVA1*.[58] Multi-omic analysis of 127 TCGA cases comparing younger with older patients and tongue with other oral sites found distinct pathway activation by age and subsite across *Rap1*, *PI3K-Akt*, *MAPK*, *cGMP-PKG*, *JAK-STAT*, and *PD-L1/PD-1* signaling, without nominating individual driver genes.[59] A separate paired-tissue study of 35 tongue and floor-of-mouth carcinomas profiled the metallothionein family, finding *MT1A*, *MT1X*, *MT3*, and *MT4* downregulated and *MT1F* upregulated; *MT1G* downregulation carried the worst prognosis, *MT1X* upregulation was restricted to non-metastatic cases and *MT3* upregulation was linked to nodal metastasis.[60]

Translation, biomarkers and reporting quality

Druggability and pharmacological validation

Fourteen of the 50 retained studies tested a compound experimentally, and all did so in cell lines, xenografts or genetically modified mice. Agents with a defined molecular target included the EZH2 inhibitor DZNep with 5-fluorouracil,[39] gamma-secretase inhibition for NOTCH1,[7] siRNA and pharmacological YAP1 inhibition,[30] rapamycin against mTOR in the K-ras/p53 mouse,[14] a CREB1 inhibitor,[45] the EGFR tyrosine kinase inhibitor EKB-569 (pelitinib) used to suppress radiation-induced NF-kappaB activation across 74 pathway molecules in SCC-4 and SCC-9 cells,[61] the combination of the FAK inhibitor Y15 with afatinib and an Axl inhibitor,[17] and the BH3-mimetic gossypol.[24] The natural compound eugenol was tested in SCC-9 with a normal keratinocyte comparator.[15] Chemotherapy and immunotherapy were tested as modulated endpoints. Cisplatin sensitivity in the BRCA1-miR-593-5p-MFF axis,[49] cisplatin with anti-PD-L1 in the syngeneic murine model,[46] and nocodazole against paclitaxel in the TTLL12 context.[37] Two pharmacological results ran counter to expectation: Src inhibition with dasatinib or PP2 reproduced, not reversed integrin alphaVbeta3-mediated multidrug resistance in CAL-27 clones,[19] and EZH2 knockout increased.[40] The remaining 36 studies proposed therapeutic targets without pharmacological testing.

Biomarker discovery

A proliferation- and mitosis-linked panel comprising *CDK1*, *CCNA2*, *TOP2A*, *SENP1* and *MAD2L1* has been proposed as a candidate biomarker set shared between OTSCC and esophageal SCC.[62] Four of the 5 are canonical cell-cycle and mitotic effectors – cyclin-dependent kinase 1, cyclin A2, topoisomerase II alpha, and the mitotic checkpoint component *MAD2L1*. Yet, none of these markers has been validated as a surrogate endpoint. Across the retained evidence, no proposed biomarker – the six-gene salivary hypermethylation panel,[10] the seven-gene tongue-specific expression signature,[58] the 7 extracellular vesicle hub proteins,[36] or the ferroptosis-related trio *CA9, TNFAIP3* and *NRAS*[8] – has been shown to predict a clinical endpoint prospectively, to change in response to therapy in a manner tracking outcome, or to have been tested in an independent validation cohort of adequate size. The single exception in terms of clinical correlation, though not of surrogacy, is the BRCA1–miR-593-5p–MFF axis, which was associated retrospectively with both cisplatin response and survival in a multicenter TSCC cohort.[49] The distinction matters for trial design. Bioinformatic studies nominated the *CDK1*, *CCNA2*, *TOP2A*, *SENP1*, and *MAD2L1* panel as candidate biomarkers. No study has evaluated the panel as a surrogate endpoint, and no evidence of surrogacy exists for it.

Reporting of HPV, p53 and p16 status

Ascertainment of viral and surrogate marker status was poor across the tongue-restricted evidence base. The HPV status was not reported in the large majority of retained studies, and where viral involvement was addressed directly it was through the murine surrogate MmuPV1.[47] The p53 status was formally characterized in only a minority, principally the germline MDM4 family study,[11] the murine tongue line series[12] and the conditional Trp53 models.[13,14] p16 was more often measured as a downstream target of epigenetic silencing than as an HPV surrogate.[39] This pattern reflects the predominance of laboratory over clinical designs in tongue-specific work and precludes any synthesis stratified by viral status at this subsite.

In silico genome-wide DNA methylation analysis

Supplementary Table S1 gives, for each contrast, the number of samples retained after quality control, the number of probes retained after filtering, the number of significant differentially methylated positions, the number of significant differentially methylated regions, the split of those calls into hypermethylated and hypomethylated, the range of mean beta differences, and the range of Benjamini-Hochberg adjusted *p*-values.

Gene-level output was restricted to promoter-region calls was then intersected with the fusion-partner gene set.

Nineteen gene symbols carry both a fusion-partner assignment and a promoter hypermethylation call in tongue carcinoma: *ADH7*; *ATAD2*; *ATRX*; *CXCR5*; *ERBB4*; *HUWE1*; *ITCH*; *P2RX4*; *PTPN1*; *PTPRD*; *PTPRN2*; *PTPRZ1*; *RAD51B*; *RAD51D*; *SRGAP2*; *TFDP1*; *TFDP2*; *TIAM1*; and *UBE3C*. No gene symbol carries both a fusion-partner assignment and a promoter hypomethylation call.

Discussion

Fusion frequency at this subsite has not been established. No denominator by sample number is available for the tongue or for the comparator subsites. The wider genetic literature at this subsite is correspondingly sparse. Across 50 tongue-attributable studies, not one recurrent somatic driver was reported consistently, and the only genome-wide copy number resource specific to the tongue was a panel of 18 cell lines.[38] An absence of this kind is not itself evidence of an epigenetic mechanism, but it makes the hypothesis worth testing.

Two earlier studies addressed the molecular characteristics of oral tongue carcinoma specifically, and the position of the present work relative to them should be stated explicitly. Krishnan et al. profiled 52 oral tongue tumors with matched controls on the 450K array and derived a minimal signature of 16 differentially methylated regions, validated against the head and neck cohort of TCGA. Their comparator was matched normal tissue, and their question was tumor against normal within one subsite. Wang et al. integrated gene expression profiles across multiple oral tongue cohorts and reported expression characteristics attributed to the subsite. Their evidence is transcriptomic and carries no methylation component. Neither study set oral tongue carcinoma against carcinoma of other oral cavity subsites profiled on the same platform. Neither placed methylation output alongside the gene set disrupted by rearrangement in fusion-positive oral cancer.

Transcription regulations compound the landscape

The evidence should be read in order of how directly each finding functions as a comparison. The most direct is PAX5 promoter methylation, which was associated with the tongue subsite within a single 93-patient oral SCC cohort analyzed on one platform[6]: the tongue and non-tongue cases were drawn from the same series and assayed identically, so the subsite contrast is internal to the study. Two further findings establish a tongue-specific signature without benchmarking it against other non-tongue subsites in the same material. The seven-gene expression set – *MTFR1*, *C8ORF33*, *OTUD6B*, *NUDCD1*, *PRKC1*, *ANO1*, and *PIK3CA* – was distinguished from an HPV-associated comparator set,[58] and the six-gene salivary hypermethylation panel – *A2BP1*, *ANK1*, *ALDH1A2*, *GFRA1*, *TTYH1*, and *PDE4B* – was validated against the TCGA oral tongue cohort, that is, against more tongue tumors.[10] Both are informative about the tongue; neither settles whether the signature is peculiar to it. The OTSCC-specific amplifications at 6q12-q14, 9p24, 11p12-p13, 11q13 and 14q24 add structural characterization of the same type.[38] Only 50 of the 197 extracted records resolved the tongue as a separate subsite, and of those, the number that placed the tongue alongside another oral-cavity subsite in the same experiment is smaller still.

The transcriptional regulators recurring across the retained evidence are *TP53*, *FOXO4*, *HIF1A*, *SOX9*, *CREB1*, *TCF12*, *Twist*, *Snai2*, *PAX5*, *WT1*, and *GATA5*, together with the unnamed master regulators identified by methylation-based enhancer analysis.[42] They appear in the p53 axis, in EMT, in the hypoxic and metabolic response, in the immune microenvironment and in the methylation findings alike. Heterogeneity in TSCC operates at the level of the individual factor, while convergence operates at the level of the output: many different transcriptional inputs, a few shared functional endpoints. *CREB1* driving macrophage mimicry,[45] *TCF12* suppressed by miR-211,[48] *SOX9* and *HIF1A* induced downstream of BMI1[41] and Snai2 induced on loss of *MTUS1*[33] are unrelated events that nonetheless terminate in proliferation, invasion or metabolic shift. The p53 pathway remained the most frequently implicated axis overall, and TERT promoter mutation recurred at a defined frequency of at least 15% in a pan-cancer survey that included TSCC among the TERT-high types.[16] Yet *TP53* status itself was characterized in a minority of retained studies, and conditional mouse genetics indicates that p53 loss is permissive.[13,14]

NOTCH1 provides the clearest instance of genuine biological heterogeneity. Forced expression of the intracellular Notch1 domain suppressed growth in Tca8113 cells,[29] while in 68 early-stage TSCC tumors *NOTCH1* was amplified and overexpressed with an inactivating mutation rate of only 4%, and both gamma-secretase inhibition and shRNA knockdown supported an oncogenic role.[7] These are not contradictory measurements of the same quantity: one is a gain-of-function experiment in an immortalized line, the other an observation in primary human tumors with loss-of-function validation. The direction of *NOTCH1* effect depends on the context in which it is assayed, and that context-dependence is a property of the biology, not an artefact of the literature. The same lesson attaches to EZH2, where overexpression in xenografts and conditional knockout in mice produced opposite phenotypes.[39,40]

Whether any of these is modified by viral status cannot be determined. Human papillomavirus was not reported in most retained studies, p16 was more often measured as a target of epigenetic silencing than as a viral surrogate, and the only direct interrogation of viral oncogene activity at this subsite used a murine papillomavirus, where

infection acted as a cofactor with chemical carcinogen exposure.[47] Harmonized HPV, p53 and p16 ascertainment is the single most straightforward improvement available to future tongue-specific studies.

Non-coding RNA and the missing arms of competing-endogenous-RNA regulation

Non-coding RNA regulation feeds into the same axes implicated by protein-coding evidence. *LINC00152* sponging miR-193b-3p activates PI3K/AKT[21]; miR-211 acts through TCF12 on a transcriptional axis[48]; miR-498 and miR-940 act through focal adhesion and ECM-receptor interaction[50]; miR-134 tracks E-cadherin loss[46]; and the BRCA1–miR-593-5p–MFF axis acts on mitochondrial fission and cisplatin sensitivity.[49] This last is the only microRNA finding in the tongue-restricted evidence with a demonstrated clinical correlate, and it is the natural candidate for prospective evaluation. That candidacy is candidacy for prospective evaluation as a correlate, and not for microRNA-directed therapy. Target multiplicity is the obstacle. A single microRNA represses many transcripts simultaneously, and any therapeutic manipulation of it acts on the whole target set. A single transcript is in turn repressed by several microRNAs, so removal of one leaves the others in place. Consequences at the remaining targets are unmeasured in every microRNA study retained here, and no microRNA-directed agent has been tested in TSCC in any retained record. The biological role of these microRNAs and their therapeutic potential are accordingly treated as separate claims throughout, and the second does not follow from the first.

Two gaps deserve comment, because they bear directly on the second research question. First, patient-tissue microRNA profiling in the tongue rests on a single 50-pair series,[9] whereas the oral-cavity comparator literature contains several larger microRNA panels, of which only miR-184 overlaps with the tongue-specific list. The reasonable inference is that the microRNA literature has not been resolved by subsite, not that the tongue lacks microRNA involvement. Second, pseudogenes and circular RNAs were absent from the tongue-attributable evidence entirely, the sole circular RNA finding anywhere in the extraction table coming from the comparator cluster.[57]

Translational and druggability implications

The translational position is unfavorable. Only 14 of the 50 retained studies tested a compound at all. The remaining 36 nominated targets without testing them. Against that background, the two counter-expectation results carry disproportionate weight as cautionary evidence for trial design. Src inhibition with dasatinib or PP2 reproduced and conditional *EZH2* knockout increased the incidence of invasive carcinoma.[40] Both involve agent classes in active clinical development, and both indicate that the direction of pharmacological effect at this subsite cannot be assumed from target biology established elsewhere. The methylation panels occupy a different translational niche: salivary detection with AUC of at least 0.800 points toward non-invasive diagnosis and surveillance.[10] However, no marker at this subsite has been validated as a surrogate endpoint, and prognostic association should not be reported as though it were.

Limitations

As an in silico study, tongue arrays derive predominantly from a single GEO series on a single platform, so analytical group and series of origin are close to collinear for the subsite contrasts. ComBat protects the biological term specified in the model matrix, and it cannot separate a biological effect from a technical one where the two are collinear. Results from the subsite contrasts are therefore reported as exploratory. A definitive test requires tongue and non-tongue oral carcinomas profiled within one series, in one laboratory, on one array generation, with subsite recorded in the deposited metadata. Further, the comparator cluster is heterogeneous by construction. It contains oral cavity and head and neck cohorts without subsite resolution, carcinomas of non-tongue subsites, and non-neoplastic material. Comparisons drawn against it are comparisons against a literature, not against a matched control series, and they carry the reporting practices of that literature with them. Design category, internal comparator and orthogonal validation were recorded instead, and these 3 items carry the whole weight of methodological appraisal here.

Moreover, array-based methylation measurement covers a fixed probe set and returns no information outside it, so promoter regions absent from the common 450K and EPIC feature set are unassessed. Tongue-attributable microRNA evidence from patient tissue rests on one series of 50 tumor-margin pairs, so subsite-resolved microRNA conclusions remain provisional. The HPV, p53 and p16 status were unreported in the majority of retained studies, which precludes any stratification of the synthesis by viral status.

Conclusions

Relative to SCC arising elsewhere in the oral cavity, OTSCC lacks recurrent somatic driver, and recurrent fusion events. Wherever studies resolved the tongue as a separate subsite, they returned tongue-specific methylation and expression markers, and methylation is accordingly the most promising axis on which to test divergence of TSCC from SCC at other oral-cavity subsites. The evidence assembled here does not establish that divergence. Within TSCC, heterogeneity arises less from variation at the level of individual genes than from multiple distinct

molecular routes converging on a small number of shared functional endpoints. Long non-coding RNAs contribute through competing-endogenous-RNA networks that feed into the same PI3K–AKT, p53 and EMT axes implicated by protein-coding evidence. Pseudogenes and circular RNAs were absent from the reviewed literature. Transcription factor disruption funnels into cell-cycle control, hypoxic-metabolic reprogramming and EMT.

On the present evidence, OTSCC is best described as a subsite carrying a candidate epigenetic signature. Designation as a distinct entity should follow a comparison of subsites profiled within one series, in one laboratory, on one array generation. That comparison has not yet been reported, and the present work does not supply it.

Ethics approval and consent to participate

Not applicable.

Data availability

The datasets supporting the findings of the current study, including all supplementary materials, are available from the corresponding author on reasonable request.

Consent for publication

Not applicable.

Use of AI and AI-assisted technologies

Not applicable.

ORCID iDs

Bacem Othman https://orcid.org/0009-0006-5567-6771
Omid Moztarzadeh https://orcid.org/0000-0002-4768-2382
Lukas Hauer https://orcid.org/0000-0001-6639-2690

References

1. Grajewski L, Greiner A, Wurschi G, et al. Challenges in recurrent head and neck squamous cell cancer treatment: Systematic review and meta-analysis comparing efficacy and toxicity between post-operative and definitive IMRT-based reirradiation. *Clin Transl Radiat Oncol*. 2025;56:101061. doi:10.1016/j.ctro.2025.101061
2. Silva JP, Pinto B, Monteiro L, Silva PM, Bousbaa H. Combination therapy as a promising way to fight oral cancer. *Pharmaceutics*. 2023;15(6):1653. doi:10.3390/pharmaceutics15061653
3. Astsaturov I, Cohen RB, Harari PM. EGFR-targeting monoclonal antibodies in head and neck cancer. *Curr Cancer Drug Targets*. 2006;6(8):691–710. doi:10.2174/156800906779010191
4. Teng Z, Teng L, Xie J. IAPs in cancers: Molecular mechanisms, clinical prognostic value, and translational therapeutic potential. *J Transl Med*. 2026;24(1):143. doi:10.1186/s12967-025-07640-7
5. Kong S, Zhang J, Wang L, et al. Mechanisms of low MHC I expression and strategies for targeting MHC I with small molecules in cancer immunotherapy. *Cancer Lett*. 2025;611:217432. doi:10.1016/j.canlet.2024.217432
6. Ribeiro IP, Caramelo F, Marques F, et al. WT1, MSH6, GATA5 and PAX5 as epigenetic oral squamous cell carcinoma biomarkers – a short report. *Cell Oncol (Dordr)*. 2016;39(6):573–582. doi:10.1007/s13402-016-0293-5
7. Upadhyay P, Nair S, Kaur E, et al. Notch pathway activation is essential for maintenance of stem-like cells in early tongue cancer. *Oncotarget*. 2016;7(31):50437–50449. doi:10.18632/oncotarget.10419
8. Zhu H, Tao Y, Huang Q, et al. Identification of ferroptosis-related genes as potential biomarkers of tongue squamous cell carcinoma using an integrated bioinformatics approach. *FEBS Open Bio*. 2022;12(2):412–429. doi:10.1002/2211-5463.13348
9. Ghffari M, Asadi M, Shanaehbandi D, et al. Aberrant expression of miR-103, miR-184, miR-378, miR-497 and miR-506 in tumor tissue from patients with oral squamous cell carcinoma regulates the clinical picture of the patients. *Asian Pacific J Cancer Prev*. 2020;21(5):1311–1315. doi:10.31557/APJCP.2020.21.5.1311
10. Rapado-González Ó, Costa-Fraga N, Bao-Caamano A, et al. Genome-wide DNA methylation profiling in tongue squamous cell carcinoma. *Oral Dis*. 2024;30(2):259–271. doi:10.1111/odi.14444
11. Toufektchan E, Lejour V, Durand R, et al. Germline mutation of *MDM4*, a major p53 regulator, in a familial syndrome of defective telomere maintenance. *Sci Adv*. 2020;6(15):eaay3511. doi:10.1126/sciadv.aay3511
12. Chen YF, Liu CJ, Lin LH, et al. Establishing of mouse oral carcinoma cell lines derived from transgenic mice and their use as syngeneic tumorigenesis models. *BMC Cancer*. 2019;19(1):281. doi:10.1186/s12885-019-5486-7
13. Kishimoto K, Kanazawa K, Nomura M, et al. Ppp6c deficiency accelerates K-ras^{G12D}-induced tongue carcinogenesis. *Cancer Med*. 2021;10(13):4451–4464. doi:10.1002/cam4.3962
14. Raimondi AR, Molinolo A, Gutkind JS. Rapamycin prevents early onset of tumorigenesis in an oral-specific K-ras and p53 two-hit carcinogenesis model. *Cancer Res*. 2009;69(10):4159–4166. doi:10.1158/0008-5472.CAN-08-4645
15. Issa H, Loubaki L, Al Amri A, et al. Eugenol as a potential adjuvant therapy for gingival squamous cell carcinoma. *Sci Rep*. 2024;14(1):10958. doi:10.1038/s41598-024-60754-8
16. Killela PJ, Reitman ZJ, Jiao Y, et al. TERT promoter mutations occur frequently in gliomas and a subset of tumors derived from cells with low rates of self-renewal. *Proc Natl Acad Sci U S A*. 2013;110(15):6021–6026. doi:10.1073/pnas.1303607110
17. Lucarini V, Angiolini V, Nardozi D, et al. In vitro synergistic effect of AXL, FAK and ErbB receptors inhibitors for head and neck cancer. *Biol Direct*. 2025;20(1):77. doi:10.1186/s13062-025-00668-1
18. Xia J, Lv N, Hong Y, et al. Increased expression of focal adhesion kinase correlates with cellular proliferation and apoptosis during 4-nitroquinoline-1-oxide-induced rat tongue carcinogenesis. *J Oral Pathol Med*. 2009;38(6):524–529. doi:10.1111/j.1600-0714.2008.00728.x
19. Stojanović N, Brozovic A, Majhen D, et al. Integrin αvβ3 expression in tongue squamous carcinoma cells Cal27 confers anticancer drug resistance through loss of pSrc(Y418). *Biochim Biophys Acta*. 2016;1863(8):1969–1978. doi:10.1016/j.bbamcr.2016.04.019
20. Kou XX, Hao T, Meng Z, Zhou YH, Gan YH. Acetylated sp1 inhibits PTEN expression through binding to PTEN core promoter and recruitment of HDAC1 and promotes cancer cell migration and invasion. *Carcinogenesis*. 2013;34(1):58–67. doi:10.1093/carcin/bgs336
21. Li X, Rui B, Cao Y, Gong X, Li H. Long non-coding RNA LINC00152 acts as a sponge of miRNA-193b-3p to promote tongue squamous cell carcinoma progression. *Oncol Lett*. 2020;19(3):2035–2042. doi:10.3892/ol.2020.11293
22. Wu Q, Zheng Z, Zhang J, et al. Chordin-like 1 regulates epithelial-to-mesenchymal transition and metastasis via the MAPK signaling pathway in oral squamous cell carcinoma. *Front Oncol*. 2022;12:862751. doi:10.3389/fonc.2022.862751
23. Lu Y, Shen Y, Li L, et al. Clinicopathological significance of FOXO4 expression and correlation with Prx1 in head and neck squamous cell carcinoma. *Anal Cell Pathol (Amst)*. 2021;2021:5510753. doi:10.1155/2021/5510753
24. Benvenuto M, Mattera R, Masuelli L, et al. (±)-Gossypol induces apoptosis and autophagy in head and neck carcinoma cell lines and inhibits the growth of transplanted salivary gland cancer cells in BALB/c mice. *Int J Food Sci Nutr*. 2017;68(3):298–312. doi:10.1080/09637486.2016.1236077
25. Schneider FT, Schänzer A, Czupalla CJ, et al. Sonic hedgehog acts as a negative regulator of {beta}-catenin signaling in the adult tongue epithelium. *Am J Pathol*. 2010;177(1):404–414. doi:10.2353/ajpath.2010.091079

26. Lin KY, Kao SH, Lai CM, et al. Tumor suppressor Lzap suppresses Wnt/β-catenin signaling to promote zebrafish embryonic ventral cell fates via the suppression of inhibitory phosphorylation of glycogen synthase kinase 3. *J Biol Chem*. 2015;290(50):29808–29819. doi:10.1074/jbc.M115.669309
27. Li L, Chapman K, Hu X, Wong A, Pasdar M. Modulation of the oncogenic potential of β-catenin by the subcellular distribution of plakoglobin. *Mol Carcinog*. 2007;46(10):824–838. doi:10.1002/mc.20310
28. Yu M, Wu G, Chen Y, Wang H, Gao Y, Wang A. Bioinformatic screening and experimental analysis identify SFRP1 as a prognostic biomarker for tongue squamous cell carcinomas. *Arch Oral Biol*. 2020:104587;110. doi:10.1016/j.archoralbio.2019.104587
29. Duan L, Yao J, Wu X, Fan M. Growth suppression induced by Notch1 activation involves Wnt-β-catenin down-regulation in human tongue carcinoma cells. *Biol Cell*. 2006;98(8):479–490. doi:10.1042/BC20060020
30. Omori H, Nishio M, Masuda M, et al. YAP1 is a potent driver of the onset and progression of oral squamous cell carcinoma. *Sci Adv*. 2020;6(12):eeay3324. doi:10.1126/sciadv.aay3324
31. Zhang H, Tang Z, Deng C, et al. HMGA2 is associated with the aggressiveness of tongue squamous cell carcinoma. *Oral Dis*. 2017;23(2):255–264. doi:10.1111/odi.12608
32. Paccione RJ, Miyazaki H, Patel V, et al. Keratin down-regulation in vimentin-positive cancer cells is reversible by vimentin RNA interference, which inhibits growth and motility. *Mol Cancer Ther*. 2008;7(9):2894–2903. doi:10.1158/1535-7163.MCT-08-0450
33. Zhao T, He Q, Liu Z, Ding X, Zhou X, Wang A. Angiotensin II type 2 receptor-interacting protein 3a suppresses proliferation, migration and invasion in tongue squamous cell carcinoma via the extracellular signal-regulated kinase–Snai2 pathway. *Oncol Lett*. 2016;11(1):340-344. doi:10.3892/ol.2015.3898
34. Zhong Z, Zhang H, Hong M, et al. FNDC3B promotes epithelial–mesenchymal transition in tongue squamous cell carcinoma cells in a hypoxic microenvironment. *Oncol Rep*. 2018;39(4):1853–1859. doi:10.3892/or.2018.6231
35. Pérez-Valencia JA, Prosdocimi F, Cesari IM, et al. Angiogenesis and evading immune destruction are the main related transcriptomic characteristics to the invasive process of oral tongue cancer. *Sci Rep*. 2018;8(1):2007. doi:10.1038/s41598-017-19010-5
36. Busso-Lopes AF, Carnielli CM, Winck FV, et al. A reductionist approach using primary and metastatic cell-derived extracellular vesicles reveals hub proteins associated with oral cancer prognosis. *Mol Cell Proteomics*. 2021;20:100118. doi:10.1016/j.mcpro.2021.100118
37. Xue L, Zeng Y, Fang C, Cheng W, Li Y. Effect of TTLL12 on tubulin tyrosine nitration as a novel target for screening anticancer drugs in vitro. *Oncol Lett*. 2020;20(6):340. doi:10.3892/ol.2020.12203
38. Järvinen AK, Autio R, Kilpinen S, et al. High-resolution copy number and gene expression microarray analyses of head and neck squamous cell carcinoma cell lines of tongue and larynx. *Genes Chromosomes Cancer*. 2008;47(6):500–509. doi:10.1002/gcc.20551
39. Li Z, Wang Y, Qiu J, et al. The polycomb group protein EZH2 is a novel therapeutic target in tongue cancer. *Oncotarget*. 2013;4(12):2532–2549. doi:10.18632/oncotarget.1503
40. Baquero J, Tang XH, Scognamiglio T, Gudas LJ. EZH2 knockout in oral cavity basal epithelia causes more invasive squamous cell carcinomas. *Carcinogenesis*. 2021;42(12):1485–1495. doi:10.1093/carcin/bgab091
41. Baquero J, Tang XH, Galke D, et al. Exogenous BMI1 expression aggravates oral squamous cell carcinomas in tongue epithelia. *Neoplasia*. 2025;62:101146. doi:10.1016/j.neo.2025.101146
42. Okano LM, Maciel da Fonseca LM, Erthal ID, Malta TM. Epigenomic integrative analysis pinpoint master regulator transcription factors associated with tumorigenesis in squamous cell carcinoma of oral tongue. *Genet Mol Biol*. 2023;46(2):e20220358. doi:10.1590/1678-4685-GMB-2022-0358
43. Zhang Z, Wang C, Sun Z, et al. CAV2-expressing nerves induce metabolic switch toward mitochondrial oxidative phosphorylation to promote cancer stemness. *Nat Commun*. 2026;17(1):203. doi:10.1038/s41467-025-66914-2
44. Song Y, Sun R, Ji J, et al. N4BP1 is essential for the development of oral cancer via controlling both cancer cells and immune microenvironment. *Cell Death Dis*. 2026;17(1):23. doi:10.1038/s41419-025-08229-0
45. Lu X, Lin W, Zheng J, et al. Sodium nitrite orchestrates macrophage mimicry of tongue squamous carcinoma cells to drive lymphatic metastasis. *Br J Cancer*. 2025;132(4):340–353. doi:10.1038/s41416-024-02923-0
46. Chen YF, Chang KW, Yang IT, Tu HF, Lin SC. Establishment of syngeneic murine model for oral cancer therapy. *Oral Oncol*. 2019;95:194–201. doi:10.1016/j.oraloncology.2019.06.026
47. Wei T, Buehler D, Ward-Shaw E, Lambert PF. An infection-based murine model for papillomavirus-associated head and neck cancer. *mBio*. 2020;11(3):e00908–e00920. doi:10.1128/mBio.00908-20
48. Chen YF, Yang CC, Kao SY, Liu CJ, Lin SC, Chang KW. MicroRNA-211 enhances the oncogenicity of carcinogen-induced oral carcinoma by repressing TCF12 and increasing antioxidant activity. *Cancer Res*. 2016;76(16):4872–4886. doi:10.1158/0008-5472.CAN-15-1664
49. Fan S, Liu B, Sun L, et al. Mitochondrial fission determines cisplatin sensitivity in tongue squamous cell carcinoma through the BRCA1–miR-593-5p–MFF axis. *Oncotarget*. 2015;6(17):14885–14904. doi:10.18632/oncotarget.3659
50. Korvala J, Jee K, Porkola E, et al. MicroRNA and protein profiles in invasive versus non-invasive oral tongue squamous cell carcinoma cells in vitro. *Exp Cell Res*. 2017;350(1):9–18. doi:10.1016/j.yexcr.2016.10.015
51. Avram EG, Moatar IA, Miok V, et al. Gene network analysis of the transcriptome impact of methylated microRNAs on oral squamous cell carcinoma. *Adv Clin Exp Med*. 2022;31(11):1231–1242. doi:10.17219/acem/151911
52. Li Z, Jiang C, Yuan Y. TCGA based integrated genomic analyses of ceRNA network and novel subtypes revealing potential biomarkers for the prognosis and target therapy of tongue squamous cell carcinoma. *PLoS One*. 2019;14(5):e0216834. doi:10.1371/journal.pone.0216834
53. Manikandan M, Magendhra Rao AK, Arunkumar G, Rajkumar KS, Rajaraman R, Munirajan AK. Down regulation of miR-34a and miR-143 may indirectly inhibit p53 in oral squamous cell carcinoma: A pilot study. *Asian Pacific J Cancer Prev*. 2015;16(17):7619–7625. doi:10.7314/apjcp.2015.16.17.7619
54. Manikandan M, Magendhra Rao AK, Rajkumar KS, Rajaraman R, Munirajan AK. Altered levels of miR-21, miR-125b-2*, miR-138, miR-155, miR-184, and miR-205 in oral squamous cell carcinoma and association with clinicopathological characteristics. *J Oral Pathol Med*. 2015;44(10):792–800. doi:10.1111/jop.12300
55. Manikandan M, Magendhra Rao AK, Arunkumar G, et al. Oral squamous cell carcinoma: microRNA expression profiling and integrative analyses for elucidation of tumourigenesis mechanism. *Mol Cancer*. 2016;15:28. doi:10.1186/s12943-016-0512-8
56. Stabile R, Cabezas MR, Verhagen MP, et al. The deleted in oral cancer (DOC1 aka CDK2AP1) tumor suppressor gene is downregulated in oral squamous cell carcinoma by multiple microRNAs. *Cell Death Dis*. 2023;14(5):337. doi:10.1038/s41419-023-05857-2
57. Ando T, Kasamatsu A, Kawasaki K, et al. Tumor suppressive circular RNA-102450: Development of a novel diagnostic procedure for lymph node metastasis from oral cancer. *Cancers (Basel)*. 2021;13(22):5708. doi:10.3390/cancers13225708
58. Reddy RB, Khora SS, Suresh A. Molecular prognosticators in clinically and pathologically distinct cohorts of head and neck squamous cell carcinoma – a meta-analysis approach. *PLoS One*. 2019;14(7):e0218989. doi:10.1371/journal.pone.0218989
59. Prostakishina EA, Dampilova TD, Kononova LA, et al. Molecular landscape of oral cancer in young adults. *Russ J Genet*. 2023;59(11):1190–1201. doi:10.1134/S1022795423110108
60. Brazão-Silva MT, Rodrigues MF, Eisenberg AL, et al. Metallothionein gene expression is altered in oral cancer and may predict metastasis and patient outcomes. *Histopathology*. 2015;67(3):358–367. doi:10.1111/his.12660
61. Aravindan N, Thomas Jr. CR, Aravindan S, Mohan AS, Veeraraghavan J, Natarajan M. Irreversible EGFR inhibitor EHB-569 targets low-LET γ-radiation-triggered rel orchestration and potentiates cell death in squamous cell carcinoma. *PLoS One*. 2011;6(12):e29705. doi:10.1371/journal.pone.0029705
62. Gumedag C, Atay S. Integrated analysis identifies CCNA2 as a candidate diagnostic and prognostic biomarker in oral tongue squamous cell carcinoma. *J Appl Oral Sci*. 2026;34:e20250618. doi:10.1590/1678-7765-2025-0618